

The role of the grain boundary on persistent photoconductivity in GaN

This article has been downloaded from IOPscience. Please scroll down to see the full text article.

2003 J. Phys.: Condens. Matter 15 7325

(<http://iopscience.iop.org/0953-8984/15/43/015>)

View [the table of contents for this issue](#), or go to the [journal homepage](#) for more

Download details:

IP Address: 171.66.16.125

The article was downloaded on 19/05/2010 at 17:40

Please note that [terms and conditions apply](#).

The role of the grain boundary on persistent photoconductivity in GaN

Niladri Sarkar, Subhabrata Dhar and Subhasis Ghosh

School of Physical Sciences, Jawaharlal Nehru University, New Delhi 110067, India

Received 16 May 2003

Published 17 October 2003

Online at stacks.iop.org/JPhysCM/15/7325

Abstract

We present an experimental investigation on temperature, excitation intensity and spectral dependence of persistent photoconductivity (PPC) in GaN. A grain boundary induced potential barrier is predicted to be responsible for PPC. The non-exponential nature of the PPC decay has been explained by a Gaussian distribution of capture barriers, arising from the trapped charges at the grain boundary interface. The spectral dependence of the PPC suggests the origin of PPC and the yellow luminescence band may arise from the same intrinsic defect.

1. Introduction

In recent years, gallium nitride (GaN) and its ternary alloys with Al and In have been extensively studied for their application in blue and ultraviolet light emitting devices, short wavelength lasers, and electronic devices for high power and high temperature applications [1]. This tremendous application potential originates from the wide range of direct energy band gaps from 2.4 to 6.2 eV (InN \rightarrow GaN \rightarrow AlN), the high breakdown voltage, and the high electron drift velocity. Despite technological breakthroughs in GaN growth, doping and metal–GaN contacting technologies, the development of devices is hampered by a high density of point, as well as extended, defects [2]. The nature of several defects and their effects on the optical and transport properties of GaN are not well understood. For example,

- (i) an anomalously long relaxation time of photoexcited carriers is commonly observed in GaN [3–10], but so far the microscopic origin of this phenomenon is not understood;
- (ii) extended defects, like a grain boundary or dislocation, are commonly observed in GaN [2], but their role on transport and optical properties is not well known;
- (iii) broad luminescence bands centred at 2.2 eV [11], known as the yellow luminescence band (YLB), and 2.8 eV [12], known as the blue luminescence band (BLB), are commonly observed, but so far no specific defect responsible for these luminescence bands has been identified conclusively.

It is well known that non-uniform strain due to mismatch in lattice parameters and thermal expansion coefficients between the substrate and GaN epilayers gives rise to a high density of extended defects. A columnar structure is often observed in transmission electron micrographs [2]. Grain-boundary induced potential fluctuation has been used to explain the anomalous Hall results [10, 13–15] of the dependence of mobility on carrier concentration and anomalous conductivity results [16] in the ion-implanted epitaxial layer. Wang *et al* [10] have shown that Hall mobility in undoped GaN is related to the long relaxation time of photoexcited carriers due to the presence of a charged dislocation–point-defect complex. Oh *et al* [17] have shown the existence of potential fluctuation in GaN. The strong correlation between electrical and optical properties observed in GaN has been explained by the local strain and potential fluctuation associated with point, as well as extended, defects, leading to the space-charge scattering of carriers. It has been shown experimentally [18] that edge dislocations act as radiative centres in GaN epilayers. Kotchelkov *et al* [19] have shown that the degradation of thermal properties is related to extended defects in GaN epilayers.

The role of extended defects on transport and optical properties has been studied in detail in other semiconductors [20] and it is well known that trapped charges at the grain boundary interface give rise to depletion region, which leads to a potential barrier for all transport processes. Recently, Shalish *et al* [21] have predicted a model for grain boundary controlled transport in GaN epitaxial layers grown on sapphire by assuming that the GaN material is mainly ordered polycrystal, consisting of columnar grains. In this paper, we report the observation of persistent photoconductivity (PPC) due to a grain boundary induced potential barrier. Photoinduced conductivity which persists for a long time after removal of the photoexcitation is known as PPC, which was first observed in GaAsP [22] and subsequently in other semiconductors [23]. PPC causes unwanted transient changes in emission, absorption and transport. The lifetime of optoelectronic devices is generally believed to be affected by PPC. A metal–insulator transition has been induced in Si-doped AlGaAs [24] using PPC. There are several models proposed for the origin of PPC in semiconductors. The purpose of these models is to explain how the photogenerated electrons (holes) are prevented from recombining with holes (electrons) by a barrier. In the large lattice relaxation (LLR) model [25, 26], the barrier between the photoexcited carriers and the deep impurity is believed to be the origin of PPC. In the microscopic random potential fluctuation (RPF) model [27], it has been proposed that random local potential fluctuations separate the photoexcited carriers and causes PPC. There are already several reports [3–10] on the observation of PPC in both n-type and p-type GaN. Most of the investigations on PPC in GaN are focused on the mechanism of decay kinetics. Although there are some suggestions on the microscopic origin of PPC involving different types of intrinsic defects, so far no specific defect responsible for this phenomena has been identified.

2. Experimental details

In this study we have used GaN epitaxial films grown on sapphire substrates by metal organic chemical vapour deposition (MOCVD). Prior to the growth of the epitaxial layers, a 30 nm thick GaN buffer layer was grown at 565 °C. After growing the buffer layer the substrate temperature was raised to 1000 °C for the subsequent 1.6 μm thick GaN epitaxial layers. Ti/Al Ohmic contacts were fabricated on the GaN surface for photoconductivity and Hall measurements. We chose a set of undoped n-type samples with background electron concentration 2×10^{16} – $2 \times 10^{17} \text{ cm}^{-3}$. The mobility of electrons in our samples with lowest ($2 \times 10^{16} \text{ cm}^{-3}$) and highest ($2 \times 10^{17} \text{ cm}^{-3}$) electron concentrations was found to be 50 and $150 \text{ cm}^2 \text{ V}^{-1} \text{ s}^{-1}$, respectively. Similar paradoxical observations (mobility decreases as

electron concentration decreases) have been made by several groups [13–15] in n-type GaN samples with high concentrations of extended defects, like dislocations and grain boundaries. This effect can be explained [13–15] by electron–extended-defect scattering. The low carrier mobility in low doped samples is due to strong scattering of electrons from charged extended defects, and as the electron concentration increases charged extended defects get strongly screened resulting in an increase in mobility with electron concentration. Preliminary studies using an atomic force microscope show the presence of grain boundaries in our samples. Detailed studies using a transmission electron microscope for observing grain boundaries more directly will be carried out in future. An Ar-ion laser (488 nm) and tungsten–halogen lamp dispersed with a monochromator were used for sub-band-gap photoexcitation. A He–Cd laser (325 nm) was used for above-band-gap photoexcitation. Neutral density filters were used to vary the intensity of photoexcitation. In order to perform the PPC decay measurement at different temperatures, the following sequence was used:

- (i) the sample was cooled in the dark at the desired temperature and equilibrated for 2 h, and then the sample was illuminated for photocurrent growth, and finally illumination was terminated for measuring the temporal decay of the photocurrent;
- (ii) the sample temperature was raised to 320 K and equilibrated for 2 h;
- (iii) the sample temperature was again brought down to another desired temperature and step (i) was followed.

Typically, the dark conductance of the sample was ~ 1 mS and the light intensity was adjusted such that the illuminated conductance was ~ 5 mS for PPC experiments. The photocurrent decay was measured in such a way that the whole cycle ensures identical initial conditions at each temperature. The photoluminescence (PL) spectra were collected in the wavelength region of 340–900 nm. The samples were kept in a closed cycle He refrigerator and were excited with the 325 nm laser line of the He–Cd laser. The PL signal was collected into a monochromator and detected with a UV-enhanced Si detector.

3. Experimental results and discussion

Figure 1 shows the PPC decay of a GaN sample at various temperatures with sub-band-gap photoexcitation (488 nm). The following observations were made on the relaxation of enhanced conductivity:

- (i) it persists for an extremely long time and decays faster at higher temperature, revealing a capture barrier driven relaxation process;
- (ii) it exhibits highly non-exponential decay, and does not follow either a power law or logarithmic dependence;
- (iii) it also does not follow stretched exponential relaxation ($I(t) = I(0) \exp(-t/\tau)^\beta$, where $I(0)$ is the maximum photocurrent at $t = 0$, τ is the decay time constant and β is the decay exponent) which has been claimed by several groups [4–6] without even showing a double-log–log plot ($\ln[\ln I(0) - \ln I(t)]$ versus $\ln(t)$), which should result linear dependence;
- (iv) the experimental data show a faster decay at the beginning of the process followed by a slower decay.

We have fitted the experimental data with a model based on Gaussian distribution $D(E_b)$ of capture barriers,

$$D(E_b) = \exp\left(-\frac{(E_b - E_{bo})^2}{4\sigma^2}\right), \quad (1)$$

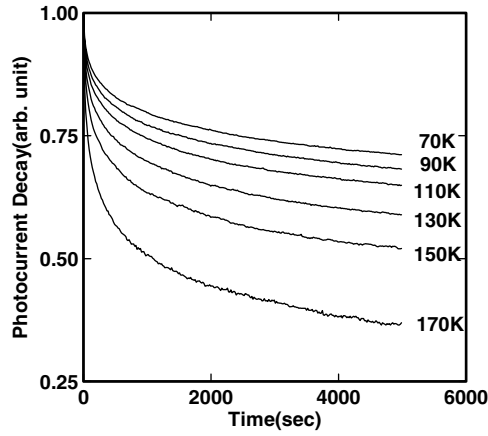


Figure 1. Photocurrent decay at different temperatures after termination of photoexcitation in a sample with background electron concentration of $5 \times 10^{16} \text{ cm}^{-3}$. The 488 nm laser line of an Ar-ion laser was used for sub-band-gap photoexcitation. Each curve is normalized to unity at $t = 0$, and the dark current has been subtracted out.

where E_{b0} is the maximum barrier height and σ is the width of the Gaussian distribution. As PPC is thermally activated, the decay constant, τ , depends on the capture barrier through the relation, $\tau = \tau_0 \exp(E_b/k_B T)$, where τ_0 is the prefactor, T is the temperature and k_B is the Boltzman constant. The decay of the enhanced conductivity can be described by the sum over all decay paths weighted with their individual probability

$$I(t) = I(0) \int_0^\infty \exp\left[-\frac{(E_b - E_{b0})^2}{4\sigma^2}\right] \exp\left[-\frac{t}{\tau(E_b)}\right] dE_b. \quad (2)$$

This model results in a fast decrease of photocurrent at the beginning of the decay due to the small capture barriers of the Gaussian distribution and a long persistent tail due to the large capture barriers of the distribution, which has also been observed by Hitsch and coworkers [6]. Figure 2 shows a $\ln(\ln I(0) - \ln I(t))$ versus $\ln(t)$ plot of PPC decay and it is evident that experimental data do not show linear dependence. The stretched exponential relaxation can reproduce only the slower part of the PPC decay, but the distributed capture barrier model explains the experimental data over the whole range of decay. The inset of figure 2 shows the distribution of the capture barriers obtained by fitting the experimental data with equation (2). In two samples with almost the same background electron concentration ($\sim 5 \times 10^{16} \text{ cm}^{-3}$), $D(E_b)$ peaks at around 135 meV (E_{b0}) with a width of 50 meV (σ) in one sample and 140 meV with the same width in another sample. The inset shows the distribution of the capture barrier determined by fitting the experimental data with equation (2).

Generally, GaN epilayers are grown on foreign substrates such as sapphire and SiC. The mismatch in lattice parameters and thermal expansion coefficient between the GaN epilayer and the substrate cause residual stress, which relaxes through the generation of a high density of extended defects. It has been shown that the interface states between grain boundaries give rise to localized energy levels inside the band gap of the semiconductor [28], and experimentally verified [29] that edge dislocations are indeed negatively charged in n-type GaN using electron holography. At thermal equilibrium some of these levels, which are below the Fermi level, are occupied with electrons, giving rise to a negative surface charge at the boundary and space charge regions on both sides of the boundary in n-type material. Essentially, the trapped charges at the grain boundary interface lead to the formation of a potential barrier for all

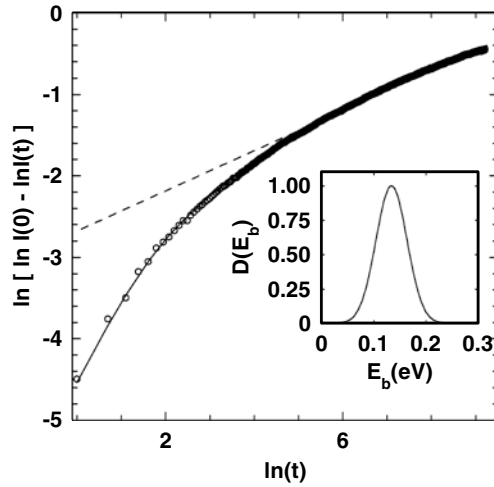


Figure 2. Comparison between the fitting of the experimental data of the photocurrent decay (empty circles) shown in figure 1 at $T = 130$ K, using equation (2) (solid curve) and using a stretched exponential (dashed line) in a $\log(\log I(0) - \log I(t))$ versus $\log(t)$ plot. The inset shows the distribution of the capture barrier determined by fitting the experimental data with equation (2).

transport processes. The barrier height can be obtained by solving the Poisson equation and is given by [20]

$$E_b = \frac{e^2 N_s^2}{8\epsilon N_D} \quad (3)$$

where N_D is the concentration of the donors inside the grain, ϵ is the dielectric constant of the semiconductor and N_s , which depends on the energetic distribution of the interface states, is the surface charge density at the grain boundary. The energetic distribution of grain boundary traps can be modelled [30] by the sum of a deep level Gaussian distribution, which gives rise to the distribution of the capture barriers. Electrons can be photoexcited to the conduction band either from defect levels lying in the forbidden gap (using sub-band-gap excitation) or from the valence band (using above-band-gap light). The photoconductivity relaxation process after removal of the photoexcitation will be different in the two cases. When the sample is illuminated with a sub-band-gap light, electrons get photoexcited to the conduction band from the interface states and immediately accumulated at the minima of the spatially fluctuating band structure. After switching off the photoexcitation, the barrier at the grain boundary will prevent photoexcited electrons from going back to their initial states, giving rise to PPC.

Figure 3 shows the PPC decay at different photoexcitation intensities of sub-band-gap light (488 nm), and as expected for the case of deep level to conduction band transitions, the PPC decay depends weakly on the excitation intensity in the case of a non-degenerate semiconductor. Caswell *et al* [31] have shown a non-exponential decay of PPC due to DX centre Si-doped AlGaAs and attributed it to an electron concentration dependent average energy of electrons in the conduction band. This is only applicable in the case of a degenerate electron system where the average energy of the electrons depends on the concentration. All our samples used in this investigations are undoped intentionally with background electron concentration of 2×10^{16} – 2.0×10^{17} cm^{-3} , which is non-degenerate over the whole temperature range (30–300 K) considered in our investigations. The inset of figure 3 shows the capture barrier (maxima of Gaussian distribution) determined from PPC decay using a different wavelength

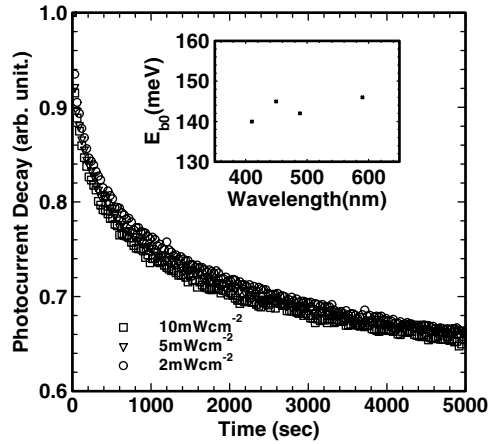


Figure 3. Photocurrent decay with different photoexcitation intensities of sub-band-gap light in a sample with background electron concentration of $5 \times 10^{16} \text{ cm}^{-3}$. The 488 nm laser line of an Ar-ion laser was used for sub-band-gap photoexcitation. Each curve is normalized to unity at $t = 0$, and the dark current has been subtracted out. The inset shows the capture barrier, E_{b0} (maxima of the Gaussian distribution) determined from photocurrent decay using different sub-band-gap light for photoexcitation.

for photoexcitation, and the near independence of the capture barrier on the wavelength of photoexcitation corroborates the distributed capture barrier model of PPC decay.

The PPC relaxation process in the case of band-to-band photoexcitation will be different from that with sub-band-gap photoexcitation. In this case, photoconductivity also persists for a long time and the rate of decay increases with temperature, but the decay kinetic is different from that in the case of sub-band-gap photoexcitation. Grain boundaries give rise to local potential fluctuation in the conduction and valence bands due to the formation of the barrier at the interfaces. When the sample is illuminated with an above-band-gap light, electrons will be photoexcited to the conduction band from the valence band, creating the same number of holes. Electrons will be redistributed at the valleys of the conduction band while holes will move toward the peaks of the valence band. In other words, electrons will accumulate at the centre, while holes will accumulate at the boundary of the grains. After the removal of photoexcitation, the photocurrent decays slowly because of the spatially indirect nature of electron–hole recombination. The rate of decay depends on the wavefunction overlap between electrons and holes. This overlap increases either with temperature, or with non-equilibrium electron–hole concentration, giving rise to a faster decay rate at higher temperature or higher excitation intensity. After photoexcitation, non-equilibrium holes will effectively change the barrier height by neutralizing some amount of negative boundary charges. Figure 4 shows the PPC with above-band-gap light (325 nm) at different intensities. The strong intensity dependence of PPC reveals the band-to-band transition. After the removal of the photoexcitation, the relaxation of the non-equilibrium photoexcited carriers n can be given by

$$\frac{dn}{dt} = -R_0 \exp\left(-\frac{E_b}{k_B T}\right) \quad (4)$$

where R_0 is the rate of electron–hole recombination in the absence of any thermal capture barrier. The barrier height E_b will depend upon the non-equilibrium electron concentration in

the conduction band, and after photoexcitation, the barrier height becomes

$$E_b = \frac{e^2(N_s^0 - n\delta)^2}{8\epsilon N_D} \quad (5)$$

where N_s^0 is the areal density of the surface charges, δ is the effective thickness of the surface layer and $N_s^0 - n\delta$ is the effective negative surface charge concentration. Now, equation (4) becomes

$$\frac{dn}{dt} = -R_0 \exp\left(-\frac{e^2(N_s^{02} + n^2\delta^2 - 2N_s^0 n\delta)}{8\epsilon N_D k_B T}\right). \quad (6)$$

After neglecting the squared term ($n^2\delta^2$), equation (6) reduces to the following form, which has an analytical solution:

$$\frac{dn}{dt} = -\Re_0 \exp\left(-\frac{2N_s^0 \delta n e^2}{8\epsilon N_D k_B T}\right) \quad (7)$$

where $\Re_0 = R_0 \exp(-e^2 N_s^{02} / 8\epsilon N_D k_B T)$ is the recombination rate at $n = 0$. The solution of equation (7) gives the relaxation of photoexcited non-equilibrium carriers and results in a logarithmic character [32]. This is a good approximation for several experimental situations [32, 33] which involve the decay of macroscopically separated photoexcited electrons and holes.

$$n = n_0 - \frac{4k_B T \epsilon N_D}{e^2 N_s^0 \delta} \ln\left(1 + \frac{At}{B}\right) = n_0 - \Lambda \ln\left(1 + \frac{t}{\tau_0}\right) \quad (8)$$

where n_0 is the initial stationary concentration just before the removal of the photoexcitation. $\Lambda = 4k_B T \epsilon N_D / e^2 N_s^0 \delta$ is a measure for the photoconductance lost within a time $\tau_0 (= B/A)$. A and B are time-independent constants and are expressed as

$$A = R_0 \exp\left(-\frac{e^2 N_s^{02}}{8\epsilon N_D k_B T}\right), \quad B = \frac{4k_B T \epsilon N_D}{e^2 N_s^0 \delta} \exp\left(-\frac{e^2 n_0 \delta N_s^0}{4\epsilon N_D k_B T}\right). \quad (9)$$

Hence, the photocurrent decay will be logarithmic, characterized with fast initial decay due to lower effective barrier height resulting from the higher value of the electron concentration. As the concentration of the electrons decreases the barrier height increases leading to a gradual decrease of the photocurrent decay rate. Similar decay kinetics have been observed in neutron-irradiated Si [34]. The solid curves in figure 4 are the fit to the experimental data with a logarithmic decay law as predicted by equation (8). The ratio A/B can be obtained by fitting the experimental data with equation (8) and can be expressed as

$$\frac{A}{B} = \frac{R_0 e^2 \delta N_s^0}{4\epsilon N_D} \exp\left(\frac{e^2 (n_0 \delta N_s^0 - N_s^{02})}{4\epsilon N_D k_B T}\right). \quad (10)$$

If we take logarithms of both sides of the above equation, we get

$$\ln\left(\frac{A}{B}\right) = \frac{e^2 \delta N_s^0}{4\epsilon \kappa N_D k_B T} n_0 + \ln\left(\frac{R_0 e^2 \delta N_s^0}{4\epsilon N_D k_B T}\right) - \frac{e^2 N_s^{02}}{4\epsilon N_D k_B T} \quad (11)$$

where n_0 will be proportional to the maximum photocurrent at $t = 0$. Parameters A and B have been determined from the fitting of the photocurrent decay for different excitation intensities. The inset of figure 4 shows the plot of $\ln(A/B)$ versus excitation intensity and their linear dependence, as predicted by equation (11), confirms the grain boundary induced local potential fluctuation in the conduction and valence bands.

There are a few reports suggesting that (i) the origin of PPC is related to YLB [7, 35, 36] and (ii) the origin of YLB is related to a grain boundary and/or dislocation [2, 37]. These

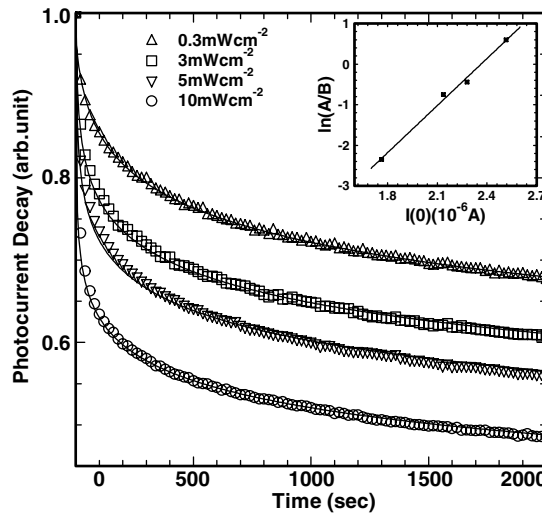


Figure 4. Photocurrent decay at $T = 100$ K with different photoexcitation intensities of above-band-gap light in the same sample as that shown in figure 1. The 325 nm laser line in a He–Cd laser was used for above-band-gap photoexcitation. Each curve is normalized to unity at $t = 0$, and the dark current has been subtracted out. The solid curves are fits to experimental data according to equation (8). The inset shows the plot of $\ln(A/B)$ (which has been obtained by fitting experimental data with equation (11) at various light intensities) versus $I(0)$, the maximum photocurrent at $t = 0$; the dark current has been subtracted out.

suggestions have been supported [7, 35, 38] by the fact that PPC is not observed in those GaN epilayers which do not show YLB. Figure 5 shows the representative PL spectra of one sample which show a strong PPC effect, shown in figure 1. PL spectra for all samples feature band edge luminescence at 3.483 eV due to donor bound exciton (BE), shallow donor–acceptor-pair (DAP) emission with zero phonon line at about 3.283 eV followed by several phonon replicas and a broad YLB peak centred at about 2.25 eV. To further strengthen the correlation between PPC and YLB, the spectral dependence of PPC has been measured. A typical spectrum obtained for this measurement is shown in figure 5. The absorption coefficient at each wavelength has been determined from photocurrent spectra using the Lambert–Beer law [39], $a(\omega) = -(1/d) \ln(1 - S(\omega)/C_S)$, where $a(\omega)$ is the absorption coefficient, $S(\omega)$ is the normalized photocurrent, d is the thickness of the sample and $C_S = S(\omega)/(1 - e^{-a(\omega)d})$. C_S is independent of photon energy [38] and was calculated [40] at $a(\hbar\omega = 3.81 \text{ eV}) = 1.55 \times 10^4 \text{ cm}^{-1}$. To get a clear threshold in the absorption spectra for different deep levels involved in the luminescence bands, we have applied the Lucovsky formula [41], which was originally proposed for absorption due to deep level defects in a semiconductor and is given by the relation $a(\omega) \propto (\hbar\omega - E_i)^{3/2}/(\hbar\omega)^3$, where E_i is the deep level energy. Figure 5 shows the transformed spectra of the variation of the absorption coefficient with photon energy. The deep level involved in the luminescence bands can be obtained by linear extrapolation of the $[\alpha(\hbar\omega)^3]^{2/3}$ as a function of photon energy $\hbar\omega$ and it is clear from figure 5 that there are two threshold at 1.45 eV, i.e. at the onset of YLB and at 2.5 eV, i.e. at the onset of BLB. The steady increase of the photocurrent over a broad range of photoexcitation reveals that the PPC comes from a distributed defect level, which is also confirmed by the distribution of the capture barrier.

The similarity in the spectral dependence between PPC and YLB is easily reconciled if one assumes that PPC is associated with YLB-related defects. It is generally believed that

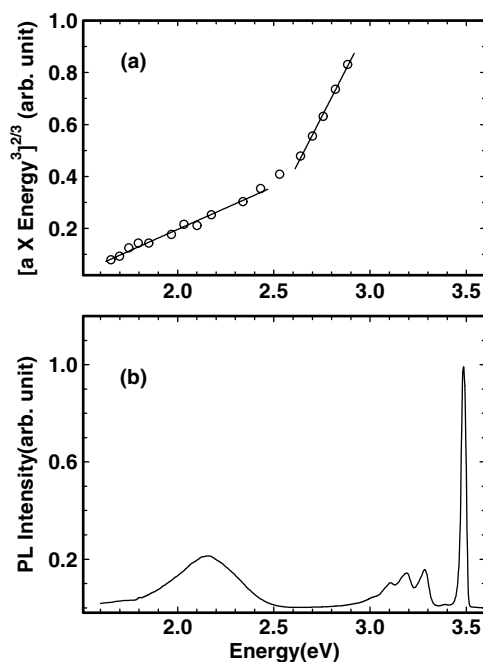


Figure 5. (a) The plot of $(a \times \text{energy}^2)^{2/3}$ versus photon energy derived from the dependence of the maximum photocurrent after 2 h of photoexcitation with different sub-band-gap light in a sample with background electron concentration of $5 \times 10^{16} \text{ cm}^{-3}$ at 30 K. (b) PL spectrum of the same sample at 10 K with excitation intensity of 100 mW cm^{-2} from a He–Cd laser (325 nm).

acceptor-type intrinsic defects are responsible for YLB. It has been shown [28] that surface states on a grain boundary and dislocation behave like acceptors, most probably due to a V_{Ga} and/or V_{Ga} -related complex, which is also predicted [11] to be responsible for YLB. Furthermore, combined cathodoluminescence and atomic force microscopic results point to extended defects in GaN as the origin of YLB. However, it is generally believed that the point defect accompanied with a strong structural relaxation due to the change in charge state is the most probable candidate for PPC. Lattice relaxation accompanied with V_{Ga} has been predicted [42] to be negligible, but this has not been verified experimentally. It is interesting to note that recent theoretical calculations [42] show that antisite defects (Ga_{N} and N_{Ga}) in GaN undergo a large outward relaxation in a different charge state from their highest symmetrical position. Ga_{N} , which is also a acceptor, and/or V_{Ga} may be responsible for both PPC and YLB, but further investigations are required to settle this issue.

4. Conclusions

In conclusion, we have observed PPC in unintentionally doped n-type GaN. The decrease of PPC decay rate with temperature reveals the capture barrier driven relaxation process. We have presented a model for grain boundary controlled transport, according to which a Gaussian distribution of the capture barrier, which results from the similar distribution of interface states at the grain boundaries, leads to the non-exponential decay of photoexcited carriers with sub-band-gap photoexcitation. In the case of band-to-band photoexcitation, the PPC relaxation follows a logarithmic decay behaviour, which has been explained in terms of a grain boundary

induced potential fluctuation in the band structure. The similar spectral dependence of PPC and YLB indicates that the defect responsible for the PPC effect may have the same microscopic origin as that of YLB.

Acknowledgments

We thank Professor J H Edgar of Kansas State University, for providing samples, and for helpful discussion and encouragement. This work was partly supported by the Council of Scientific and Industrial Research (CSIR), India. One of the authors, NS, acknowledges the support of a CSIR junior research fellowship.

References

- [1] Nakamura S and Fasol G 1997 *The Blue Laser Diode: GaN Based Light Emitters and Lasers* (New York: Springer)
- Morkoc H 1999 *Nitride Semiconductors and Devices* (New York: Springer)
- [2] Ponce F A and Bour D P 1997 *Nature* **386** 351
- [3] Johnson C, Lin J Y, Jiang H X, Khan M A and Sun C J 1996 *Appl. Phys. Lett.* **68** 1808
- [4] Qiu C H and Pankove J I 1997 *Appl. Phys. Lett.* **70** 1983
- [5] Beadie G *et al* 1997 *Appl. Phys. Lett.* **71** 1092
- [6] Hirsch M T, Wolk J A, Walukiewicz W and Haller E E 1997 *Appl. Phys. Lett.* **71** 1098
- [7] Reddy C V, Balakrishnan K, Okumura H and Yoshida S 1998 *Appl. Phys. Lett.* **73** 244
- [8] Horng H *et al* 1999 *Thin Solid Films* **343/344** 642
- [9] Seifert O P *et al* 1999 *MRS Internet J. Nitride Semicond. Res.* **4S1** G5.5
- [10] Wang W, Chua S J and Li G 2000 *J. Electron. Mater.* **29** 27
- [11] Ogino T and Aoki M 1980 *Japan. J. Appl. Phys.* **19** 2398
- Glaser E R *et al* 1995 *Phys. Rev. B* **51** 13326
- Hofmann D M *et al* 1995 *Phys. Rev. B* **52** 16702
- Suski T *et al* 1995 *Appl. Phys. Lett.* **67** 2188
- Calleja E *et al* 1997 *Phys. Rev. B* **55** 4689
- Saarinen K *et al* 1997 *Phys. Rev. Lett.* **79** 3030
- Ponce F A *et al* 1996 *Appl. Phys. Lett.* **68** 57
- Rosner S J *et al* 1997 *Appl. Phys. Lett.* **70** 420
- Lee I H *et al* 1997 *Appl. Phys. Lett.* **71** 1359
- Schubert E F, Goepfert I D and Redwing J M 1997 *Appl. Phys. Lett.* **71** 3224
- Li X, Bohn P W and Coleman J J 1999 *Appl. Phys. Lett.* **75** 4049
- Koschnick F K *et al* 2000 *Appl. Phys. Lett.* **76** 1828
- [12] Kaufmann U *et al* 1998 *Appl. Phys. Lett.* **72** 1326
- Viswanath A K *et al* 1998 *J. Appl. Phys.* **83** 2272
- Kaufmann U *et al* 1999 *Phys. Rev. B* **59** 5561
- Reschchikov M A, Yi G C and Wessels B W 1999 *Phys. Rev. B* **59** 13176
- Reshchikov M A *et al* 2000 *J. Appl. Phys.* **87** 3351
- Shahedipour F and Wessels B W 2000 *Appl. Phys. Lett.* **76** 3011
- [13] Fehrer M, Einfeldt S, Birkle U, Gollnik T and Hommel D 1998 *J. Cryst. Growth* **189/190** 763
- [14] Ng H M, Doppalapudi D, Moustakas T D, Weimann N G and Eastman L F 1998 *Appl. Phys. Lett.* **73** 821
- [15] Look D C and Szelove J R 1999 *Phys. Rev. Lett.* **82** 1237
- [16] Uzan-Sagui C *et al* 1999 *Appl. Phys. Lett.* **74** 2442
- [17] Oh E *et al* 1998 *Appl. Phys. Lett.* **72** 1848
- [18] Hino T *et al* 2000 *Appl. Phys. Lett.* **76** 3421
- [19] Kotchelkov K *et al* 2001 *Appl. Phys. Lett.* **79** 4316
- [20] Orton J W and Powell M J 1980 *Rep. Prog. Phys.* **43** 1263
- [21] Shalish I *et al* 2000 *Phys. Rev. B* **61** 15573
- [22] Craford M G, Stillman G E, Rossi J A and Holonyak N 1968 *Phys. Rev.* **168** 867
- [23] Kakalios J and Fritzsche H 1984 *Phys. Rev. Lett.* **53** 1602
- Hundgausen M and Ley L 1985 *Phys. Rev. B* **32** 6655
- Choi S H, Yoo B S and Lee C 1987 *Phys. Rev. B* **36** 6479
- Jiang H X and Lin J Y 1990 *Phys. Rev. B* **41** 5178

- [24] Katsumoto S *et al* 1988 *J. Phys. Soc. Japan* **56** 2257
- [25] Lang D V, Logan R A and Jaros M 1979 *Phys. Rev. B* **19** 1015
- [26] Ghosh S and Kumar V 1993 *Europhys. Lett.* **24** 779
- [27] Sheinkman M K and Shik Y A 1976 *Sov. Phys.—Semicond.* **10** 128
- [28] Elsner J *et al* 1998 *Phys. Rev. B* **58** 12571
- [29] Cherns D and Jiao C G 2001 *Phys. Rev. Lett.* **87** 205504
- [30] Dimitriadis C A, Tassis D H, Economou N A and Lowe A J 1993 *J. Appl. Phys.* **74** 2919
- [31] Caswell N S, Mooney P M, Wright S L and Solomon P M 1986 *Appl. Phys. Lett.* **48** 1093
- [32] Shik A Y 1977 *Sov. Phys.—Semicond.* **11** 1030
Shik A Y 1995 *Electronic Properties of Inhomogeneous Semiconductors* (London: Gordon and Breach)
- [33] Quisser H J and Theodorou D E 1979 *Phys. Rev. Lett.* **43** 401
Quisser H J and Theodorou D E 1986 *Phys. Rev. B* **33** 4027
- [34] Gregory B L 1970 *Appl. Phys. Lett.* **16** 67
- [35] Chen H M, Chen Y F, Lee M C and Feng M S 1997 *Phys. Rev. B* **56** 6942
Chen H M, Chen Y F, Lee M C and Feng M S 1997 *J. Appl. Phys.* **82** 899
- [36] Chung S J *et al* 2001 *J. Appl. Phys.* **89** 5454
- [37] Ponce F A, Bour D P, Gotz W and Wright P J 1996 *Appl. Phys. Lett.* **68** 57
Rosner S J, Carr E C, Ludowise M J, Gorolami G and Erikson H I 1997 *Appl. Phys. Lett.* **70** 420
- [38] Li J Z, Lin J Y, Jiang H X, Khan M A, Salvador A, Botchkarev A and Morkoc H 1996 *Appl. Phys. Lett.* **69** 1474
- [39] Korntizer K *et al* 1998 *J. Appl. Phys.* **83** 4397
- [40] Manaresi M O 1996 *Phys. Rev. B* **53** 16425
- [41] Lucovsky G 1966 *Bull. Am. Phys. Soc.* **11** 206
- [42] Mattila T, Seitsonen A P and Nieminen R M 1996 *Phys. Rev. B* **54** 1474
Gorczyca I, Svane A and Christensen N E 1999 *Phys. Rev. B* **60** 8147